

Saturday, October 14 | 3:15 pm–4:45 pm | Platform Session 3

3:30 pm
Real-Time Label-Free Imaging of Dynamic Metabolic Processes During Apoptosis In Live Cells
Marina Marjanovic¹, Andrew Bower¹, Joanne Li¹, Eric Chaney¹, and Stephen Boppart¹
¹University of Illinois at Urbana-Champaign, Urbana, IL

3:45 pm
Improved Performance in Fiber Bundle Imaging Systems Via Dithering
Arthur Gmitro¹, Andrew Rouse¹, and Neil Momsen¹
¹University of Arizona, Tucson, AZ

4:00 pm
Photonic Inactivation of Virus Particles by Femtosecond Lasers
Mina Nazari¹, Rahm Gummuluru¹, Mi Hong¹, Björn Reinhard¹, and Shyamsunder Erramilli¹
¹Boston University, Boston, MA

4:15 pm
Noncontact 3-dimensional Speckle Contrast Diffuse Correlation Tomography of Tissue Blood Flow Distribution
Mingjun Zhao¹, Chong Huang¹, Daniel Irwin¹, Siavash Mazdeyasna¹, Nneamaka Agochukwu¹, Ruohui Li^{1,2}, Lesley Wong¹, and Guoqiang Yu¹
¹University of Kentucky, Lexington, KY, ²Beijing Union University, Beijing, China, People's Republic of

4:30 Pm
Accurate Segmentation of Pressure Ulcer Images
Ahmed Shalaby¹, Ali Mahmoud¹, Begoña García-Zapirain², Adel Elmaghraby¹, and Ayman El-Baz¹
¹University of Louisville, Louisville, KY, ²EVIDA Research Group,Deusto University, Spain, Deusto, Spain

OP-Sat-3-9 **Room 228A**
Track: Device Technologies and Biomedical Robotics
Affordable Health and Frugal Innovation
Chairs: Adam Brown, Perry Weinthal

3:15 pm
Automating Biomarker Concentration and Signal Enhancement for Paper-Based Chlamydia Detection
Daniel Bradbury¹, April Pan¹, Benjamin Wu^{1,2}, and Daniel Kamei¹
¹University of California Los Angeles, Los Angeles, CA, ²School of Dentistry, University of California Los Angeles, Los Angeles, CA

3:30 pm
Measuring the Mass, Volume, and Density of Microgram-Sized Objects in Fluids
Shirin Mesbah Oskui¹, Heran Bhakta¹, Graciél Diamante¹, Huinan Liu¹, Daniel Schlenk¹, and William Grover¹
¹University of California, Riverside, Riverside, CA

3:45 pm
Implementation of a Split Trehalase in an Electrochemical Biosensor for Rapid Point-of-Care Detection of Antibodies and Biomarkers of Disease
Jeroen De Buck¹ and Marija Drikic¹
¹University of Calgary, Calgary, AB, Canada

4:00 pm
Rapid Workflow for Cancer Cell Genomics
Adam Snider¹ and Anubhav Tripathi¹
¹Brown University, Providence, RI

4:15 pm
Open-Source Device for Variable Ulnar Eminence
Perry Weinthal¹
¹Florida Atlantic University, Boca Raton, FL

4:30 pm
Point-of-Care System for Monitoring Cellular Adhesion in Sickle Cell Disease
Mark Lewandowski¹, Jonathon Koss¹, Jane Little¹, and Umut Gurkan¹
¹Case Western Reserve University, Cleveland, OH

OP-Sat-3-10 **Room 226A**
Track: Bioinformatics, Computational and Systems Biology
Analysis of Cell Signaling
Chairs: Megan McClean, Princess Imoukhuede

3:15 pm
A Rule-based Model of the CamKII Holoenzyme
Matthew Pharris¹, Melanie Stefan², and Tamara Kinzer-Ursem¹
¹Purdue University, West Lafayette, IN, ²The University of Edinburgh, Edinburgh, United Kingdom

3:30 pm
How Specific Sequence Features of FG Nups Affect Nucleocytoplasmic Transport
Mohaddeseh Peyro¹, Mohammad Soheilypour¹, Ali Ghavami¹, Briana Lee¹, and Mohammad Mofrad¹
¹University of California Berkeley, Berkeley, CA

3:45 pm
Keratinocyte ERK Signaling is Modulated by Growth Factor Presentation Scheme and Cellular Tight Junctions
Pamela Kreeger¹, Chloe Kim¹, Sarah Jacobsen¹, Cameron Stewart¹, Megan McClean¹, and Kristyn Masters¹
¹University of Wisconsin-Madison, Madison, WI

4:00 pm
Computational Model Predicts the Dynamics of Thrombospondin-1 Mediated Apoptosis Signaling
Qianhui Wu¹, Jennifer Rohrs¹, Pin Wang¹, and Stacey Finley¹
¹University of Southern California, Los Angeles, CA

Saturday, October 14 | 3:15 pm–4:45 pm | Platform Session 3

4:15 pm
Large-scale Logic-based Differential Equation Computational Model Revealed a New Dimension in Macrophage Polarization
Xiaji Liu¹, Jingyuan Zhang¹, Angela Zeigler¹, Merry Lindsey^{2,3}, and Jeffrey Saucerman¹
¹University of Virginia, Charlottesville, VA, ²University of Mississippi Medical Center, Jackson, MS, ³G.V. (Sonny) Montgomery Veterans Affairs Medical Center, Jackson, MS

4:30 pm
High-dimensional Single-cell Signaling Analysis Identifies Novel Targets for Eradicating Latent HIV-infected T Cells
Linda Fong¹ and Kathryn Miller-Jensen¹
¹Yale University, New Haven, CT

OP-Sat-3-11 **Room 226B**
Track: Neural Engineering
CNS Repair and Regeneration
Chairs: Stephanie Seidlits, Ryan Koppes

3:15 pm
Improving Functional Gains in a Skilled Reaching Task Following Brain Injury Through Combinatorial Neural Stem Cell and Motor Rehabilitation Therapy
Caroline Addington¹, Gergey Mousa², Peter Hillebrand², Amber Bengson², Kristen Okada², Akshara Thakore², Sarah Stabenfeldt², and Jeffrey Kleim²
¹University of Virginia, Charlottesville, VA, ²Arizona State University, Tempe, AZ

3:30 pm
Endogenous Neural Stem Cell Activation After Traumatic Brain Injury
Jeremy Anderson¹, Misaal Patel¹, Quinn Wade¹, Kelvin Kwan¹, and Li Cai¹
¹Rutgers University, Piscataway, NJ

3:45 pm
Feasibility of Nanoparticle Delivery Correlates With Blood Brain Barrier Permeability After Diffuse Brain Injury
Vimala Bharadwaj¹, Rachel Rowe², Jordan Harrison², Chen Wu², Trent Anderson², Jonathan Lifshitz^{2,3}, P. David Adelson³, Vikram Kodibagkar¹, and Sarah Stabenfeldt¹
¹Arizona State University, Tempe, AZ, ²University of Arizona, College of Medicine-Phoenix, Phoenix, AZ, ³Barrow Neurological Institute at Phoenix Children's Hospital, Phoenix, AZ

4:00 pm
Implantation of an Astrocyte Extracelllular Matrix Containing Hydrogel Improves Neural Fiber Growth into a Spinal Cord Lesion
Russell Thompson^{1,2}, Jennifer Pardieck^{1,2}, Lindsey Crawford², and Shelly Sakiyama-Elbert¹
¹University of Texas-Austin, Austin, TX, ²Washington University in St Louis, St Louis, MO

4:15 pm
IL-4-Releasing Films Shift Macrophages to an Anti-inflammatory State for Spinal Cord Injury Regeneration
Alexis Ziemba¹, Anthony D'Amato¹, Devan Puhl¹, Taylor MacEwen¹, Abigail Koppes², Ryan Gilbert¹, Michelle Lennartz³, and Ryan Koppes²
¹Rensselaer Polytechnic Institute, Troy, NY, ²Northeastern University, Boston, MA, ³Albany Medical Center, Albany, NY

4:30 pm
Combinatorial Lentiviral Gene Delivery of Pro-oligodendrogenic Factors to Improve Myelination of Regenerating Axons After Spinal Cord Injury
Dominique Smith¹, Daniel Margul², Mitchell Johnson¹, and Lonnie Shea¹
¹University of Michigan - Ann Arbor, Ann Arbor, MI, ²Northwestern University, Chicago, IL

OP-Sat-3-12 **Room 227C**
Track: Undergraduate Research, Design & Leadership
Undergraduate Research, Design & Leadership III
Chairs: Jeffrey La Belle, Tim Becker

3:15 pm
The Influences of Mitochondrial Depolarization on Mitochondrial Network Structures
Shao-Ting Chiu¹, Jun-Yi Leu², and An-Chi Wei¹
¹Department of Electrical Engineering, National Taiwan University, Taipei, Taiwan, ²Institute of Molecular Biology, Academia Sinica, Taipei, Taiwan

3:24 pm
3-Dimensional Fluid-Structure Interaction Computational Model of Heart Valves for Bioreactor Optimization
Frederic Blais¹, Giulia Luraghi², Francesco Migliavacca², Giancarlo Pennati², Leslie Sierad^{1,3}, and Ethan Kung¹
¹Clemson University, Clemson, SC, ²Politecnico di Milano, Milan, Italy, ³Aptus Bioreactors, Clemson, SC

3:33 pm
Antibacterial Effects of Copper-PDMS Membranes for Artificial Lungs
Angela Lai¹, Neha Kapate¹, Neil Carleton¹, and Keith Cook¹
¹Carnegie Mellon University, Pittsburgh, PA

3:42 pm
Similarity in Viral and Host Promoters Couples Viral Reactivation with Host Cell Migration
Kathrin Bohn-Wippert¹, Erin Tevonian¹, Melina Megaridis¹, and Roy Dar¹
¹University of Illinois at Urbana-Champagin, Urbana, IL

The Influences of Mitochondrial Depolarization on Mitochondrial Network Structures

Shao-Ting Chiu¹, Jun-Yi Leu², and An-Chi Wei¹

¹Department of Electrical Engineering, National Taiwan University, Taipei, Taiwan,

²Institute of Molecular Biology, Academia Sinica, Taipei, Taiwan

Introduction: The mitochondrial life cycle includes fission and fusion, which contribute to the dynamic morphology. Besides, mounting evidence indicates that mitochondrial fusion process avoids damaged mitochondria from fusing with others based on mitochondrial membrane potential. However, how mitochondrial damage influences mitochondrial network remains unclear. In this study, we first depolarized mitochondria by uncoupler, and investigated changes of mitochondrial 3D structure from a network point of view. Also, we have implemented an artificial neural network for automatic recognition of damaged mitochondrial network. This study provides insights into morphological response to mitochondrial damage and possible application to clinical diagnosis.

Materials and Methods: *S. cerevisiae* S288C labeled with Kgd1-GFP was used for mitochondrial imaging. Cells were treated with 10 μ M FCCP (carbonylcyanide-p-trifluoromethoxyphenylhydrazone), a mitochondrial uncoupler, for 50 min to depolarize mitochondria, and the untreated cells are regarded as the control. Mitochondrial 3D images were captured by a Delta Vision microscope, and processed by MitoGraph software (Fig. 1A). We further calculated network features including network density (the ratio of actual connections to potential connections), average and variance of mitochondrial length, network size (number of nodes). The comparison for two groups was calculated by Mann-Whitney U test. Moreover, we have constructed a full-connected neural network with two hidden layers to classify mitochondrial morphology into two groups.

Results and Discussion: Network density, average and variance of mitochondrial length decrease significantly after FCCP treatment (Fig. 1B), while the network size increases significantly compared to the untreated population. The slower fusion rate of damaged mitochondria may contribute to increased nodes and decreased connections in the mitochondrial network, which result in lower network density and higher size. The fragmentation may also result in lower average and variance of mitochondrial length in the damaged network. The implemented neural network performs at 68% accuracy (Fig. 1C), applying deep learning framework may improve the performance.

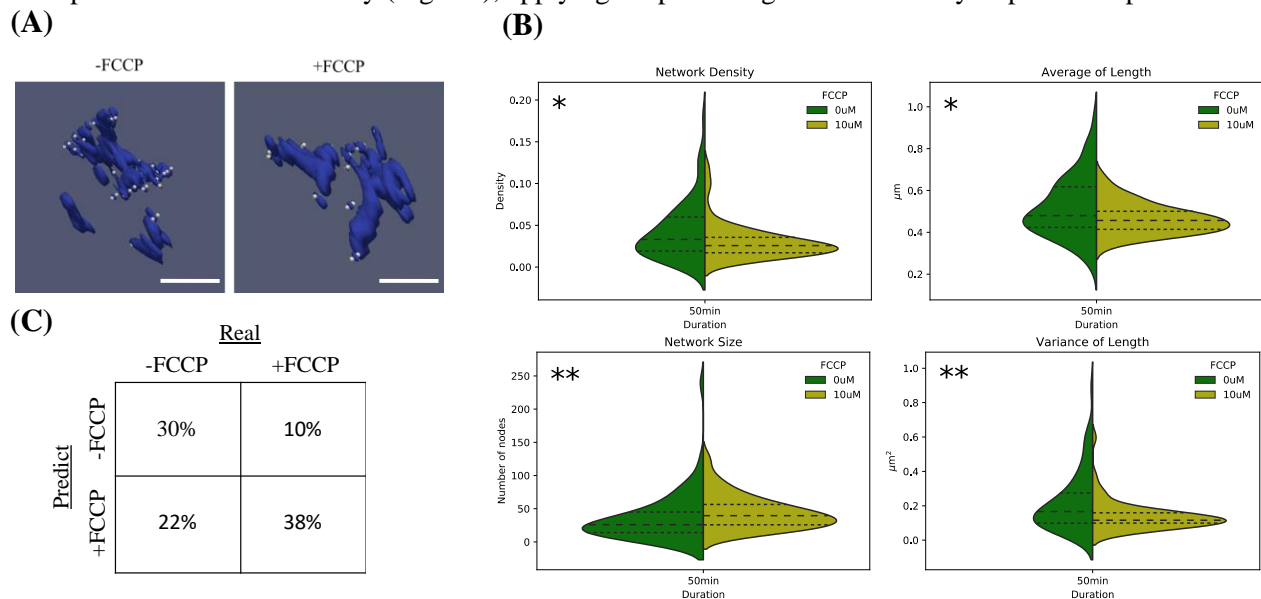


Fig. 1. (A) Mitochondrial morphology with or without FCCP treatment (10 μ M). Blue part represents the mitochondrial surface, and white part represents the mitochondrial skeleton. Scale bars represent 2 μ m (B) The effect of FCCP treatment to the mitochondrial network (n=126). *P < 0.05 and **P < 0.01 vs. control (Mann-Whitney U test, one-tailed) (C) Classification results. A neural network was used to classify mitochondrial status based on four mitochondrial network features (n=126).

Conclusions: The morphological changes caused by mitochondrial uncoupler includes lower density, average and variance of mitochondrial length, and higher network size. The significantly different features provide opportunities for automatic recognition of damaged mitochondrial morphology.

The Influences of Mitochondrial Depolarization on Mitochondrial Network Structures

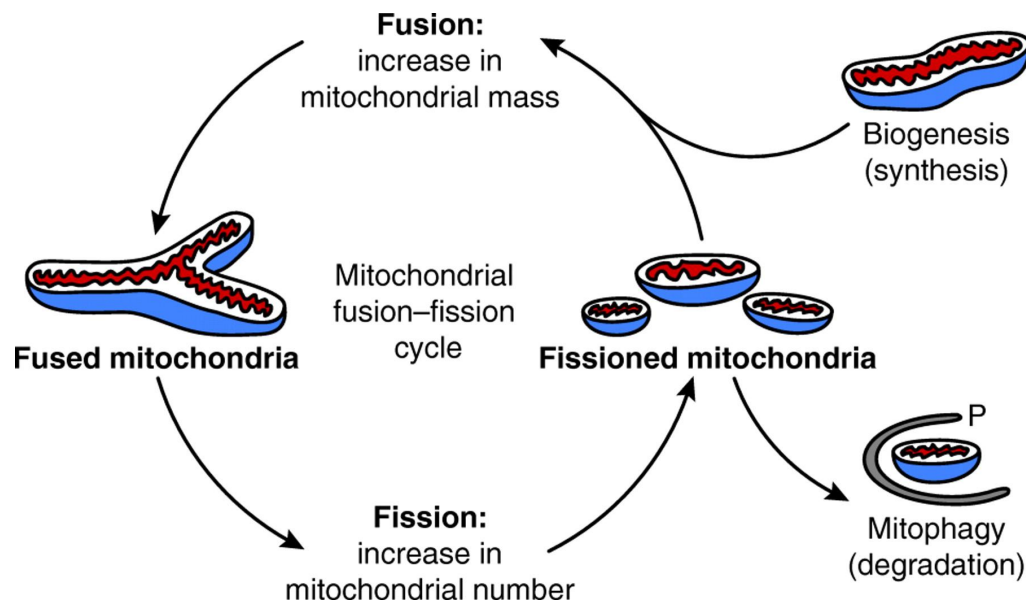
Shao-Ting Chiu

**Department of Electrical Engineering,
National Taiwan University, Taipei, Taiwan**

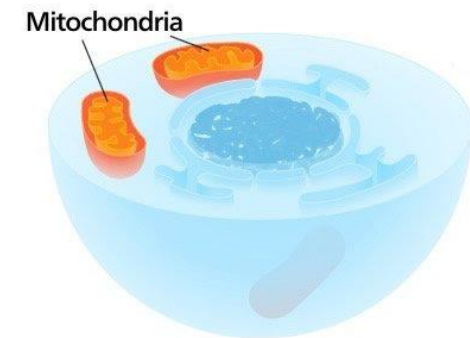
BMES 2017, Phoenix

Introduction

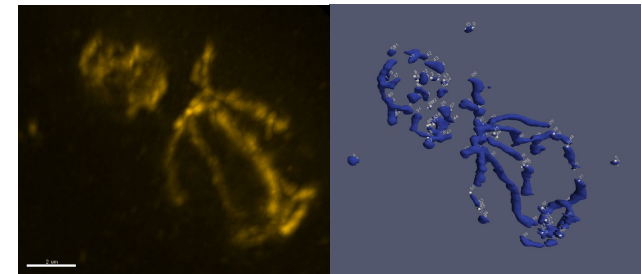
(2) Mitochondrial life cycle



(1) Mitochondria in a cell



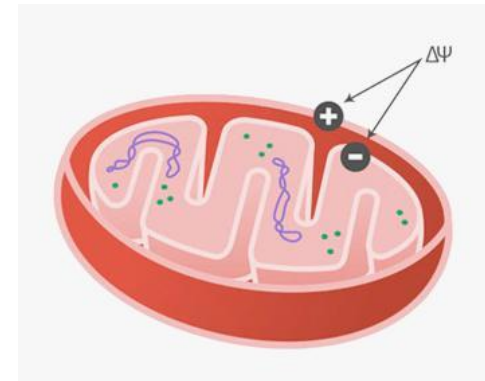
(3) Yeast mitochondrial network



(Left) 3D mitochondrial structure
(Right) Skeletonized mitochondrial network

Main Questions

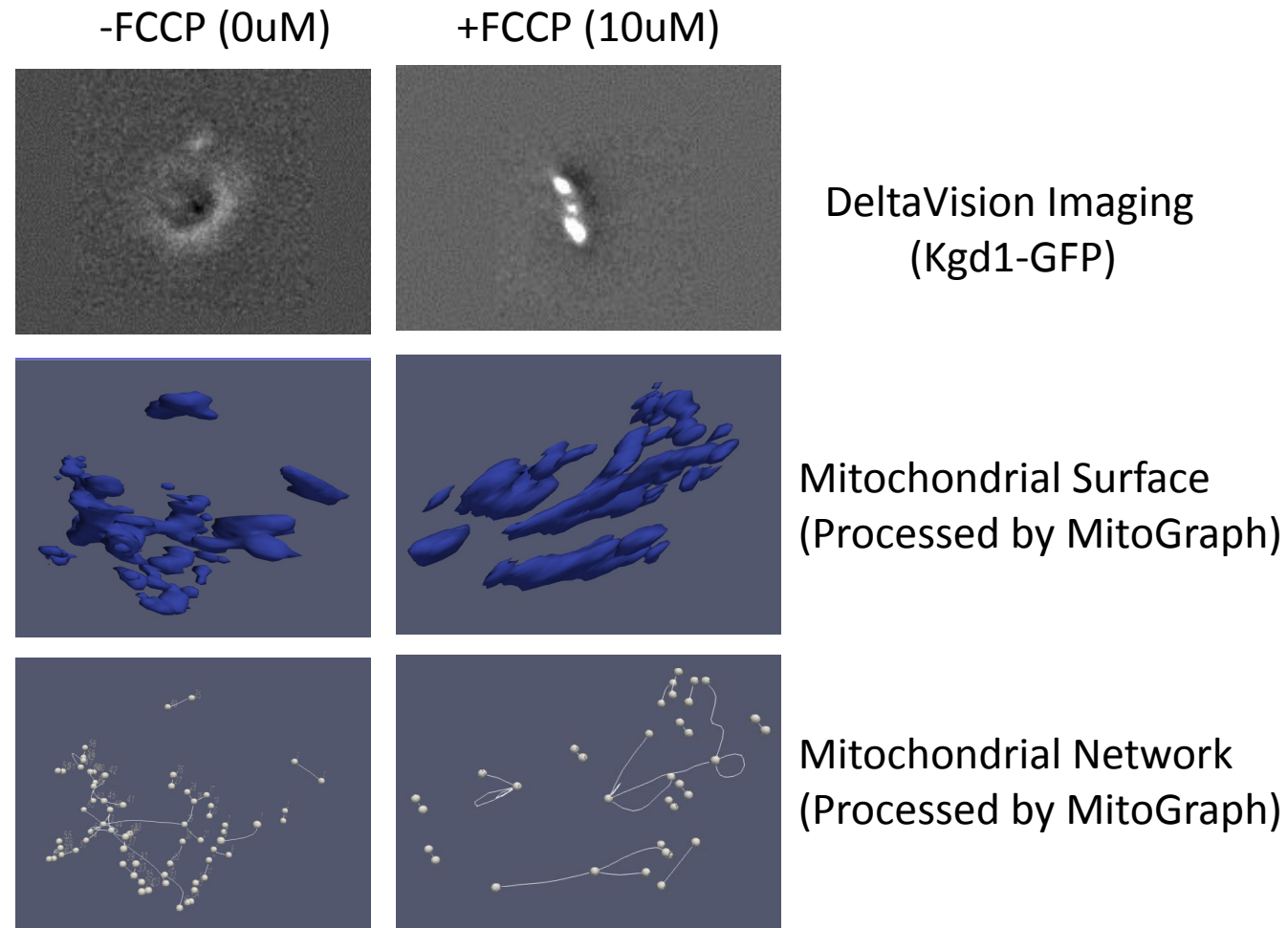
- What are the differences between normal and depolarized mitochondrial network?
 - Graph theory provides useful features to distinguish mitochondrial morphology
- How to predict depolarization based on mitochondrial morphology?



Mitochondrial membrane potential

Figure from ThermoFisher Website

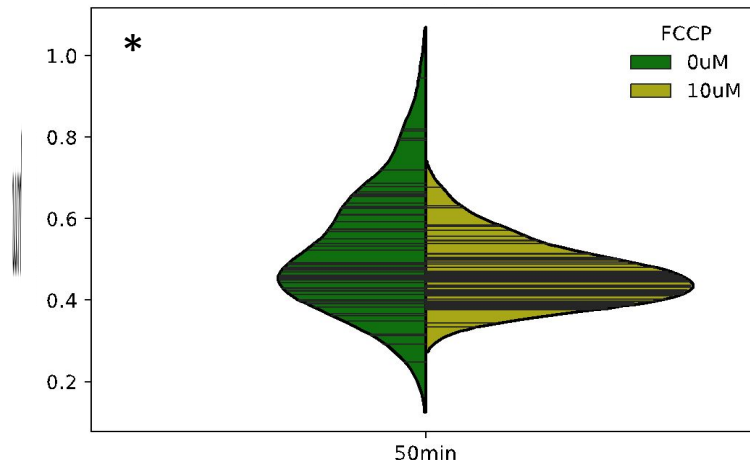
Yeast Mitochondrial 3D Imaging and Depolarization



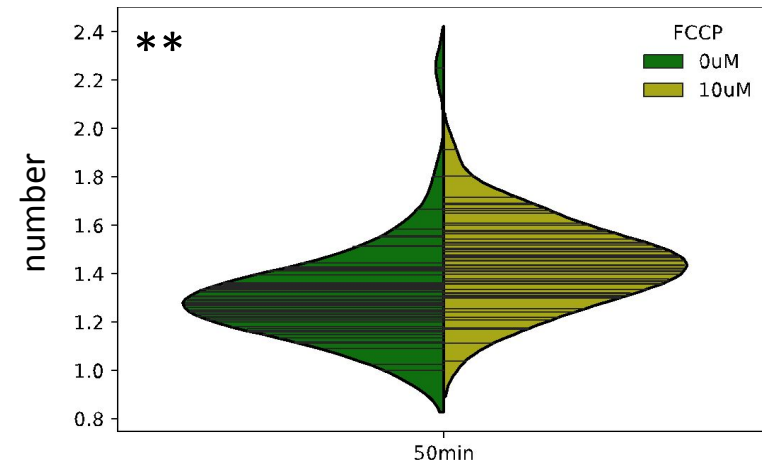
+FCCP: 10uM FCCP (uncoupler), 50 min treatment. MitoGraph software: Viana et al. Biophys. Method (2015)

Network Properties (1)

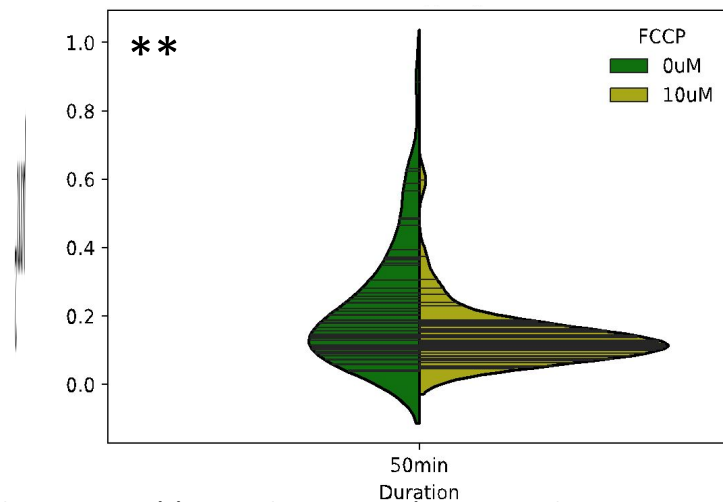
Average of Length



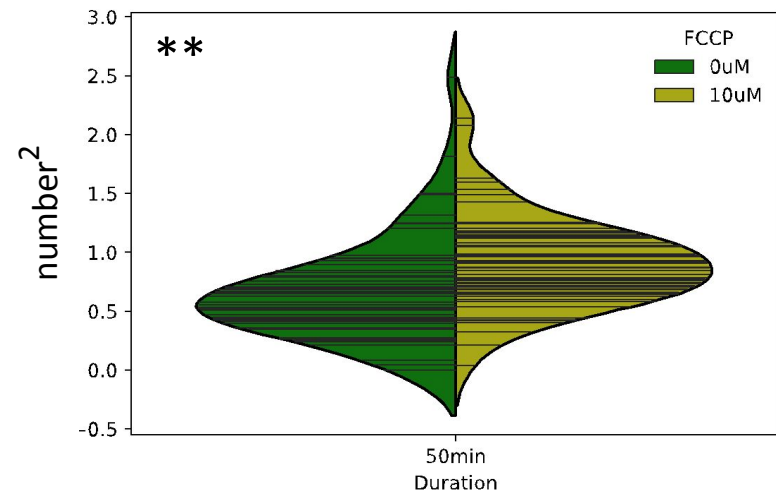
Average of Degree



Variance of Length



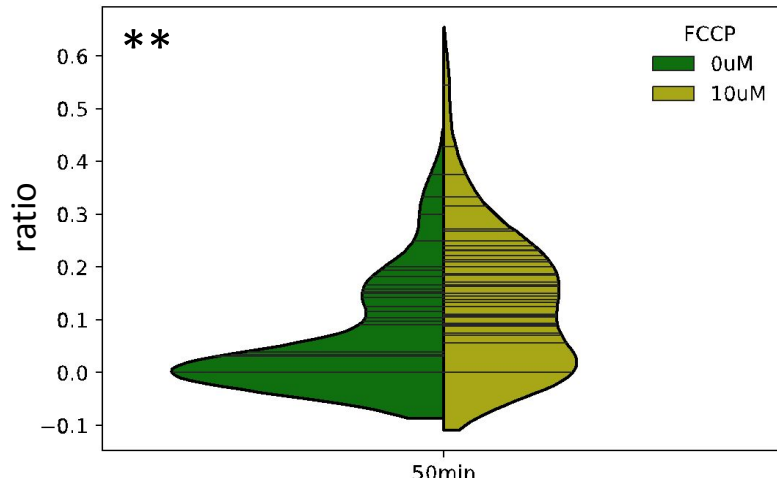
Variance of Degree



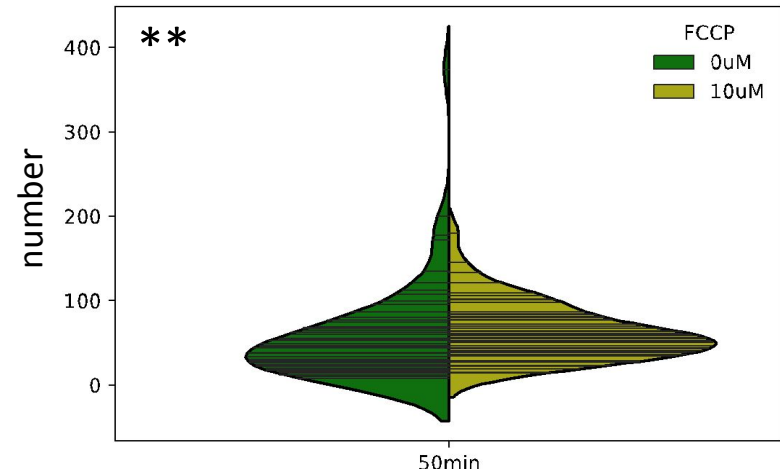
*: p value < 0.05; **: p value < 0.01 (Mann-Whitney U test, two-tailed)

Network Properties (2)

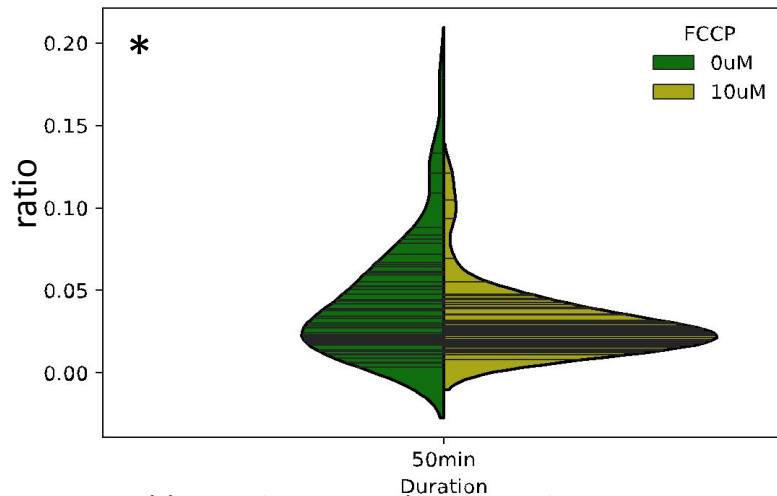
Transitivity



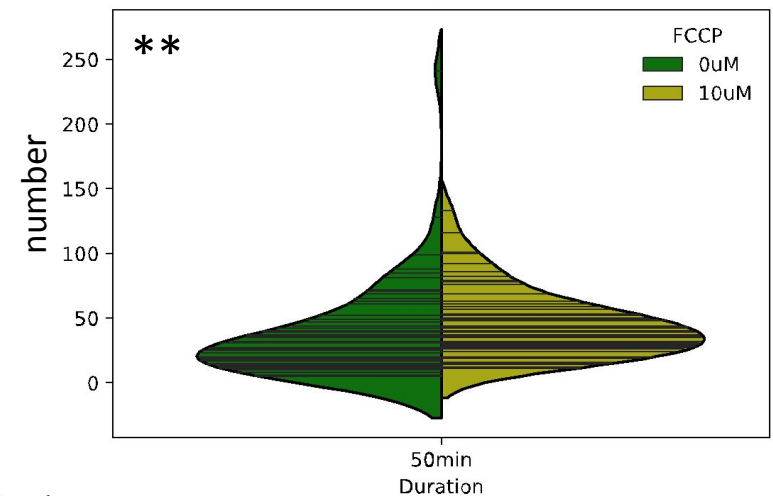
Number of Nodes



Density

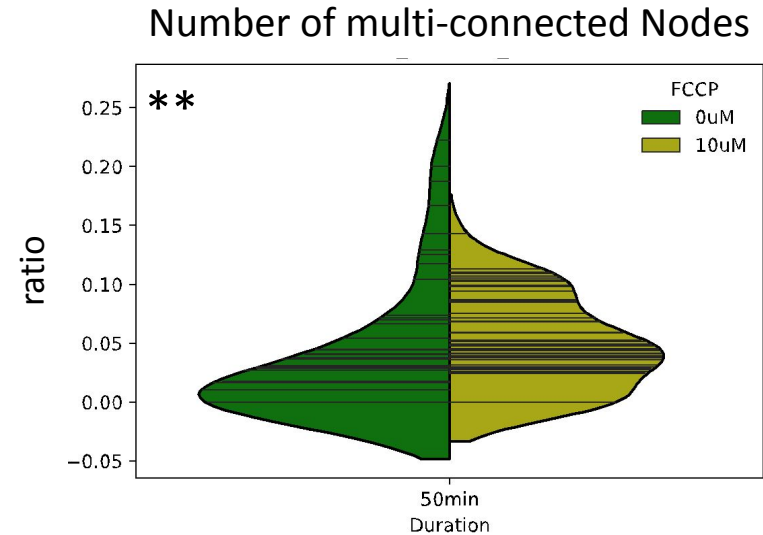
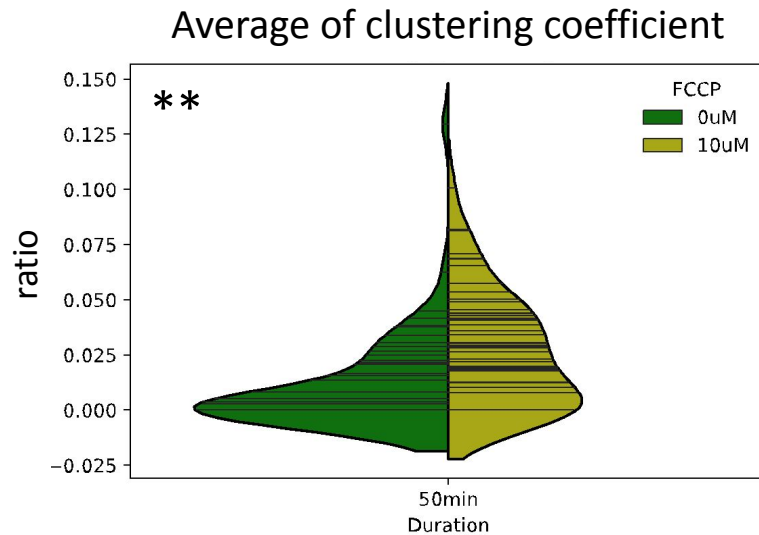


Number of Edges



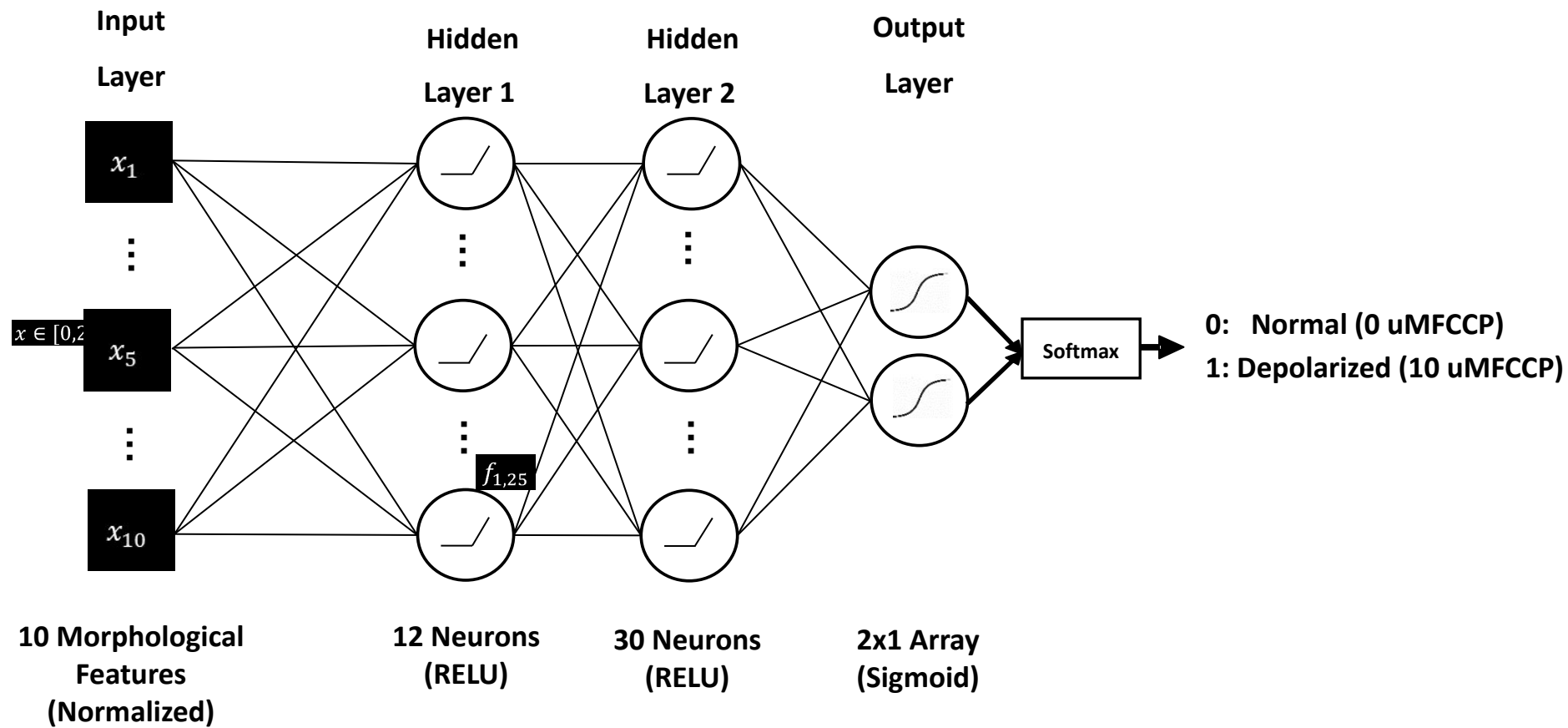
*: p value < 0.05; **: p value < 0.01 (Mann-Whitney U test, two-tailed)

Network Properties (3)



*: p value<0.05; **: p value<0.01 (Mann-Whitney U test, two-tailed)

Artificial Neural Network for Mitochondrial Depolarization Detection



Performance of Classification

- Testing accuracy: 90% (62 samples)

		<u>Predict</u>	
		-FCCP	+FCCP
<u>Real</u>	-FCCP	87%	13%
	+FCCP	0%	100%

- Training accuracy: 100% (63 samples)

Discussion

- Depolarized mitochondrial network possesses lower average and variance of length can be explained by decreased mitochondrial fusion rate.
- Though the differences of network features between normal and depolarized mitochondria are little, the combination of these features is still enough to predict the conditions.
- The main source of prediction error is from false positive (type I error).

Summary

- Normal and depolarized mitochondrial network possessed at least 10 network features in significant difference.
- Implemented Artificial neural network can predict mitochondrial depolarization based on morphological features in 90% accuracy.

Acknowledgement

- Supervisors

□ Dr. An-Chi Wei

Department of Electrical Engineering,
National Taiwan University

□ Dr. Jun-Yi Leu

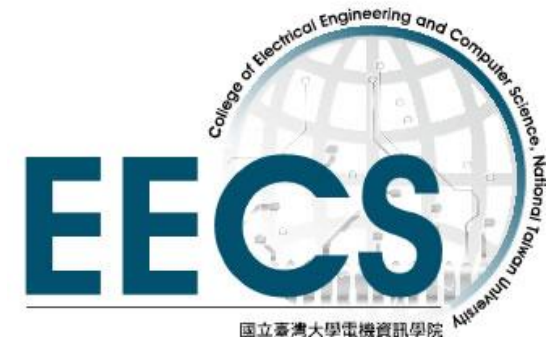
Institute of Molecular Biology,
Academia Sinica, Taipei, Taiwan

- EE Student travel fund

- Supported by



National
Taiwan
University



Supplemental Materials

G : network; V : a node; k_v : degree of V ;

N_V : Number of links between neighbors of V

- Clustering Coefficient ($C(V)$)

$$C(V) = \frac{N_V}{C_2^{k_v}}$$

- Density($D(G)$)

$$D(G) = \frac{\text{Number of edges in } G}{C_2^{\text{Number of nodes in } G}}$$

- Transitivity($T(G)$)

$$T(G) = \frac{3 \times \text{Triangles}}{C_3^{\text{Number of nodes in } G}}$$

Supplemental Materials

- Human bone osteosarcoma possesses sophisticated mitochondrial network

